Journal of Academia and Industrial Research (JAIR)
Volume 3, Issue 4 September 2014

ISSN: 2278-5213

RESEARCH ARTICLE

Equilibrium and Kinetic Adsorption Studies of Methyl Orange from Aqueous Solutions Using Kaolinite, Metakaolinite and Activated Geopolymer as Low Cost Adsorbents

Gaston Fumba, Jean Serge Essomba, Guy Merlain Tagne, Julius Ndi Nsami, Placide Désiré Bélibi Bélibi and Joseph Ketcha Mbadcam*
Physical and Theoretical Chemistry Laboratory, Department of Inorganic Chemistry,
Faculty of Science, University of Yaoundé I, Yaoundé–Cameroon
jketcha@yahoo.com*; +237 77912871

Abstract

In this study, efficiency of kaolinite (KAO), metakaolinite (MK) and activated geopolymer (GEO-7) as adsorbents for the removal of Methyl orange (MO) in aqueous solution were investigated. The parameters affecting the adsorption process such as contact time, pH, adsorbent dosage and initial dye concentration were studied. Experimental results have shown that the adsorbed amount of MO molecules increased with contact time and reached equilibrium in 15 min for KAO and GEO-7 and then 10 min for MK. The best adsorption was at pH of 2.5. To describe the equilibrium adsorption, Langmuir, Freundlich and Dubinin-Kaganer-Radushkevich (D-K-R) isotherms were used. The data fitted best Langmuir isotherm with correlation coefficient, R^2=0.995, 0.984 and 0.972 for the three adsorbents with maximum adsorption capacities of 1.247, 3.076 and 0.3393 mg/g for KAO, MK and GEO-7 respectively. Pseudo-first order, pseudo-second order, mass transfer, Elovich and intraparticule diffusion kinetic models were used to describe the kinetic process. For the kinetic model, the higher correlation value was observed for pseudo second order (R^2=0.999) confirming that chemisorption was the rate-limiting step.

Keywords: Methyl orange, adsorption, kaolinite, metakaolinite, activated geopolymer, chemisorption.

Introduction

Dyes are inherently highly visible, meaning that for concentrations as low as 0.005 ppm captures both public and authorities attention (Pierce, 1994; Hameed, 2007). Dye industry wastewater is one of the major problems. Color is one of the characteristics of an effluent which is easily detected (Nacera and Bensmaili, 2005). There are more than 10,000 commercially available dyes (Ramaraju *et al.,* 2013) with over $7x10^5$ tons of dyestuff produced and used annually; about 12 % of synthetic textiles dyes used each year are lost during manufacture and processing operations (Voudrias *et al.,* 2002; Mohammed *et al.,* 2012) and 20% of these lost dyes get into the environment through effluents from the treatment of industrial wastewater (Smaranda *et al.,* 2011). Wastewater containing dye is very difficult to treat, since the dyes are recalcitrant organic molecules, resistant to aerobic digestion and are stable to light, heat and oxidizing agents due to their structure and molecular size (Abdullah *et al.,* 2005). Some are carcinogenic and mutagenic (Supdita, 2010). Methyl orange (MO) is one of the popular dyes also known as acid orange 52. Orange III or tropaelin D is a simple model of azoic dye widely used in industrial processes such as textile and chemical products. Various methods for purification and recycling have been developed and used such as; ion exchange, chemical precipitation, electrodialysis, coprecipitation, electrolysis, membrane filtration, reverse osmosis and adsorption (Gong *et al.,* 2006; Zhang *et al.,* 2012; Almutairi *et al.,* 2012; Nsami and Mbadcam, 2013). Amongst the numerous techniques of dye removal, the cost of treated water by adsorption varies from 10 to 200 US$ per million liters (Imran and Gupta, 2006). Adsorption is a fast, inexpensive, universal method and widely applicable technique (Jain, 2005). Activated carbon is the most widely used adsorbent because it has excellent adsorption efficiency for organic compounds, but usually limited in use due to its high cost. In order to decrease the cost of treatment, attempts have been made to find inexpensive alternative adsorbents. Consequently, a number of low cost and easily available materials, such as zeolites, biosorbents, clays, agricultural and industrial wastes, manganese oxide and silica gel are effective in the colored treatment (Albanis *et al.,* 2000; Crini, 2006). In this context, kaolin clays are good source of adsorbents for the removal of various pollutants from wastewater due to their availability and low cost. The main objective of this study was to evaluate the efficiency of removal of Methyl orange from aqueous solution using kaolinite, metakaolinite and activated geopolymer as low cost adsorbents, with respect to contact time, effect of pH, adsorbent dose, initial concentration of dye, agitation on the process of dye adsorption.

Materials and methods

Preparation of adsorbate: Methyl orange (MO) was purchased from Fluka Chemika Supplier Company.

MO is an azo dye since it contain the azo group band (-N=N-). MO was applied without any further purification. Its molecular formula is $C_{14}H_{14}N_3NaO_3S$ (Fig. 1) and an index color number of C.I 13025. A stock solution of dye was prepared by dissolving 1000 mg of MO in 1000 mL of distilled water to get concentration of 1000 mg/L. The lesser concentrations of dye were obtained with dilution process.

Fig. 1. Molecular structure of methyl orange.

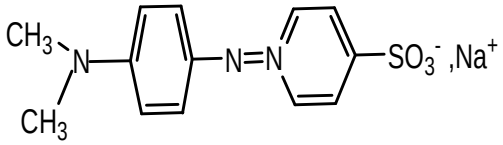

Preparation of adsorbents: Kaolinite, metakaolinite and activated geopolymer, the derivatives of kaolin clay (the principal source) were collected from Kribi; in the South Region of Cameroon. The kaolin clay was washed several times with tap water and finally with distilled water using 80 µm meshes size to remove any adhering dirt to transform it into kaolinite by removing most of the impurities. The resulting slurry was allowed to sediment and particles of sizes less than or equal to 2 µm were obtained. After complete sun dried, one part of the kaolinite was used to prepare metakaolinite. This was done by heating in a furnace at heating rate of 5°C/min up to 700°C (Elimbi *et al.,* 2011). Heating was maintained at this level of temperature for 6 h before being allowed to cool in the furnace to ambient temperature. The activated geopolymer was prepared according to the following procedure: mixing of sodium hydroxide solution (12 M) and silicate solution in the ratio of $Na_2O.SiO_2$/NaOH = 2. 440 g of metakaolinite and 300 g of the above mixture were progressively shaken slowly for 15 min followed by vigorous shaking during the last 5 min in a homogenizer M&O, model N50-G. The obtained solid was dried and then calcined at 700°C for 4 h at the rate of 5°C/min. The adsorbents were broken and ground into fine powder using a mortar and were then allowed to pass through an 80 µm mesh opening size. The sieved powder were kept in an oven at 110°C for 24 h, removed and placed in a desiccator containing $CaCl_2$ (drying agent) for 1 h. These materials (powder) were stored in airtight containers in a cool and dry place for further use.

Adsorbents characterization: Physical properties such as specific surface, pore volume distribution were measured using the nitrogen adsorption technique using surface area analyzer (TriStar 3000 V6.05A). The surface area was calculated using the BET method. Diffrap+d8 model bruker and philips equipment were used to obtain the X-ray diffraction (XRD) pattern of kaolinite, metakaolinite and activated geopolymer samples to identify their crystallinity. Infrared spectra of the three samples were measured from 400 to 4000 cm^{-1} using a bruker alpha-p spectrometer with ethanol as solvent.

The chemical analysis of the three adsorbents was obtained using Harrison method by X-ray fluorescence.

Adsorption equilibrium studies: Batch adsorption tests were carried out by adding a fixed amount of adsorbent (0.1 g) into a number of 250 mL conical flasks containing a definite volume (20 mL in each case) of different initial concentrations (10-50 mg/L) of dye solution without changing pH (2.5) at room temperature. The flasks were placed on a shaker and agitation was provided at different equilibrium times. The dye concentrations were measured using an UV-visible spectrophotometer (HACH) at 470 nm. The amount of adsorption at equilibrium, Q_e(mg/g) was calculated by:

$$Q_e = \frac{C_o - C_e}{w} xV \quad (1)$$

Where, C_o and C_e (mg/L) are the liquid-phase concentrations of dye at initial and equilibrium, respectively. V is the volume of the solution (L) and w is the mass of dry adsorbent used (g). The dye removal percentage (%R) can be calculated as follows:

$$\%R = \frac{C_o - C_e}{C_o} x100 \quad (2)$$

Where, C_o and C_e (mg/L) are the liquid-phase concentrations of dye at initial and equilibrium, respectively. The equilibrium data were then fitted by using the Langmuir, the Freundlich and Dubinin-Kaganer-Radushkevich adsorption isotherm models.

Langmuir adsorption isotherm studies: The Langmuir adsorption equation is one of the most common isotherm equations for modeling equilibrium data in solid-liquid systems. This equation is valid for monolayer adsorption onto a surface with a finite number of identical sites which are homogeneously distributed over the adsorbent surface. The general form of the Langmuir equation is (Essomba *et al.,* 2014):

$$Q_e = \frac{Q_m K_L C_e}{1 + K_L C_e} \quad (3)$$

Where, C_e is the equilibrium concentration of MO (mg/L), Q_e is the amount of MO adsorbed per unit mass of the adsorbent, K_L is the Langmuir adsorption constant (L/mg) and Q_m is the maximum amount of per unit mass of adsorbent to form a complete monolayer on the surface (mg/L). The linear form of this equation is as follows:

$$\frac{1}{Q_e} = \frac{1}{Q_m} + \frac{1}{Q_m K_L C_e} \quad (4)$$

The effect of isotherm shape can be used to predict whether an adsorption system is “favorable” or “unfavorable.” The essential features of the Langmuir isotherm can be expressed in terms of a dimensionless constant separation factor or equilibrium parameter R_L, which is defined by the following relationship (Samarghandi *et al.,* 2009):

$$R_L = \frac{1}{1+K_L C_o} \quad (5)$$

The value of R_L indicates the type of the isotherm to be either unfavorable (R_L>1), favorable (0<R_L<1) or irreversible (R_L= 0) (Mbadcam *et al*., 2012).

Freundlich adsorption isotherm: The Freundlich isotherm is the earliest known relationship describing the adsorption equation and is often expressed as:

$$Q_e = K_f C_e^{1/n} \quad (6)$$

The linear form of the Freundlich isotherm equation is:

$$Q_e = \ln K_f + (\frac{1}{n}) C_e \quad (7)$$

Where, Q_e is the quantity of MO adsorbed at equilibrium (adsorption density: mg of adsorbate per g of adsorbent). C_e is the concentration of adsorbate at equilibrium (mg/L). K_f and n are the empirical constants dependent on several factors and n is greater than one.

Dubinin-Kaganer-Radushkevich (D-K-R) isotherm studies: Langmuir and Freundlich isotherms are insufficient to explain the physical and chemical characteristics of adsorption. D-K-R isotherm is commonly used to describe the sorption isotherms of single solute systems. The D-K-R isotherm, apart from being analogue of Langmuir isotherm, is more general than Langmuir isotherm as it rejects the homogeneous surface or constant adsorption potential. The D-K-R isotherm is expressed as (Mbadcam *et al.,* 2012):

$$Q_e = Q_{max} \exp\left[\frac{\left(RT\ln\left(1+\frac{1}{Ce}\right)\right)^2}{-2Ea^2}\right] \quad (8)$$

E_a: is the main energy of adsorption and gives information about the physical and chemical features of adsorption.The linear form of the D-K-R isotherm equation is:

$$\ln Q_e = \ln Q_{max} - \beta\varepsilon^2 \quad (9)$$

Where, $\varepsilon = RT\ln(1/C_e)$ is called Polanyi potential.

Kinetic adsorption studies: In the literature, several models have been applied to know the order of the adsorbent-adsorbate interactions and the rate of adsorption of the dyes. In this study, the following five kinetic models are applied for the experimental data.

The pseudo first order model: This model assumes that the rate of change of solute uptake with time is directly proportional to difference in saturation concentration and the amount of the solid uptake with time (Raffeia *et al.,* 2012). The rate constant of adsorption is expressed as a first order rate expression as shown below:

$$\frac{dQ_t}{dt} = k_1(Q_e - Q_t) \quad (10)$$

Where, Q_e and Q_t are the sorption capacity at equilibrium and at time t respectively (mg.g^{-1}) and $k_1$is the rate constant of pseudo-first order sorption (L.min^{-1}). After integration and applying boundary conditions, t = 0 to t = t and Q_t=0 to Q_t=Q_t the integrated form of equation is:

$$\ln(Q_e - Q_t) = \ln Q_e - \frac{k_1}{2.303} t \quad (11)$$

The pseudo second order model: The rate of adsorption pseudo second order model (Theivarasu *et al*., 2011) can be given as:

$$\frac{dQ_t}{dt} = k_2(Q_e - Q_t)^2 \quad (12)$$

Where $k_2$is the rate constant of pseudo-second order sorption (g.mg^{-1}.min^{-1}). The integrated and rearranged form of equation is:

$$\frac{t}{Q_t} = \frac{1}{k_2 Q_e^2} + \frac{t}{Q_e} \quad (13)$$

Elovich equation: The Elovich equation is another rate expression in which the adsorbing surface is heterogeneous (Mbadcam *et al*., 2012):

$$\frac{dQ_t}{dt} = \alpha e^{-\beta Q_t} \quad (14)$$

Where, $\boldsymbol{\alpha}$ is the initial sorption rate (mg^{-1}.g.min^{-1}), β is the desorption constant (g.mg^{-1}) during any one experiment. The integrated and simplified equation is:

$$Q_t = \frac{\ln(\alpha\beta)}{\beta} + \frac{\ln t}{\beta} \quad (15)$$

The intraparticle diffusion model: The linear form of this equation is expressed as follows (Zora and Snezana, 2006):

$$\ln P = \ln k_{id} + a \ln t \quad (16)$$

Where, *P* is the percent removal of MO at time t, K_{id} is the intraparticular diffusion rate constant and a is gradient whose value depends on the adsorption mechanism.

Mass transfer equation: The mass transfer equation is generally expressed as (Augustine *et al.,* 2007):

$$C_o - C_t = De^{K_o t} \quad (17)$$

Where, C_o is the initial MO concentration (mg.dm^{-3}), C_t is the dye molecule concentration at time t, t is the shaking time (min), D is a fitting parameter, k_o is the adsorption constant which is related to the mass transfer adsorption coefficient. A linearized form of equation is:

$$\ln(C_O - C_t) = \ln D + k_o t \quad (18)$$

Results and discussion

Characterization studies: The XRD shows that anatase (A), illite (I), quartz (Q), kaolinite (K), and lepidocrocite (L) are the major constituents of the KAO (Fig. 2).

Fig. 2. XRD spectra of KAO, MK and GEO.7.

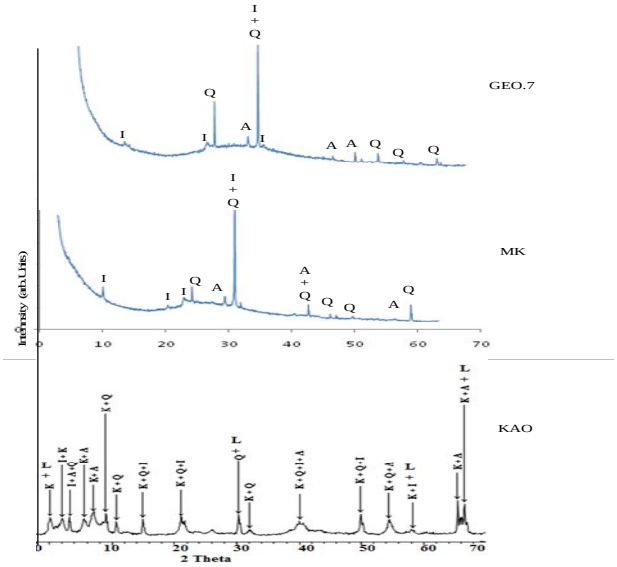

Fig. 3. FT-IR spectra of KAO, MK and GEO.7.

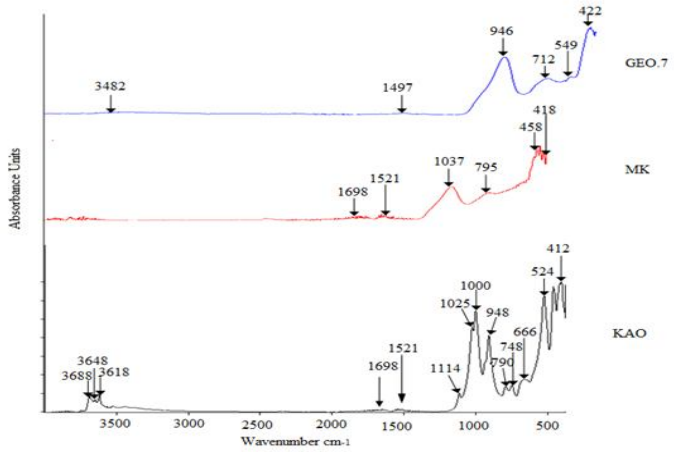

Table 1. Chemical composition of the KAO, MK and GEO.7.

Oxides (%)	KAO	MK	GEO.7
SiO_2	49.52	46.99	53.42
Al_2O_3	32.04	34.66	32.75
Na_2O	0.05	10.55	8.93
TiO_2	0.99	0.94	0.97
Fe_2O_3	0.75	0.79	0.83
K_2O	0.69	0.67	0.69
MgO	0.13	0.16	0.15
CaO	0.04	0.06	0.06
Loss on ignition	15.73	5.05	2.04
Total	99.94	99.91	99.34

MK and GEO.7 spectra show the disappearance of the more intense pick of KAO between 2Θ = 9° and 2Θ = 67°. The appearance of the intense pick of quartz on the GEO.7 spectrum also shows that quartz is the major crystalline phase in this material. In addition to these crystalline phases, these adsorbents also indicate the presence of halo of diffraction between 20° and 40° (2Θ). This shows the presence of amorphous phases in these materials. The chemical analysis of KAO, MK and GEO.7 is presented in Table 1. This shows that the major elements in our materials are SiO_2 and Al_2O_3. The high percentage of SiO_2 in the GEO.7 is due to its treatment with silicate solution during the geopolymerization step. BET measurements on the kaolinite, metakaolinite and activated geopolymer showed their surface areas to be 20.1819, 33.8331 and 35.6662 m²/g respectively. These results showed that the surface area increases with the different steps of transformation (heating and basic treatment). A FT-IR spectroscopy analysis carried out on the KAO, MK and GEO.7 powders gave functional groups as shown in Fig. 3. From the spectra, we can observe the following: kaolinite shows that the characteristic bands at 3688, 3648 and 3618 cm^{-1} correspond to O-H stretching vibrations (Saikia and Parthasarathy, 2010).

Other bands at 1114, 1025 and 1000 cm^{-1} correspond respectively to bending vibrations of Si-O; Si-O-Si and Si-O-Al. The band at 908 cm^{-1} is assigned to Al-O-H bending vibration, why bands at 790 and 748 cm^{-1} showed the presence of quartz in the sample. Metakaolinite shows that after heating of the kaolinite sample at 700°C, its characteristic bands have disappeared. This means that the kaolinite sample was successfully transformed into metakaolinite. The presence of band at 1037 cm^{-1} can be assigned to symmetric and asymmetric stretching vibrations of Si-O-Si and Si-O-Al (Elimbi *et al.,* 2011). The disappearance of the band at 908 cm^{-1}, in this case indicates the loss of the Al-O-H connection. The bands characteristic of the Si-O bond located at about 1114 and 1025 cm^{-1} seems to have been transformed into a localized intense single band at 1042 cm^{-1} (Gabche *et al.,* 2013). The 1698-1521 cm^{-1} sharp band can be ascribed to the bending mode of H_2O molecules adsorbed by metakaolinite sample. Activated geopolymer shows the band at 3482 cm^{-1} corresponds to O-H stretching vibration, this appears after 700°C of heating might be due to the humidity. The bands located at about 422-549 cm^{-1} were assigned to Si-O-Si and Al-O-Si symmetric and asymmetric stretching vibrations.

Effect of agitation time: Adsorption experiments were carried out on given solutions of MO of initial concentration 20 ppm for time interval between 5 to 40 min with pH 2.5. The experimental results obtained for the adsorption of MO during varying contact times are shown in Fig. 4. During the first 5 min, the rate of MO removal was rapid in all materials due to available sites on their surfaces. MO uptake increases with increasing agitation time within 15, 10 and 15 min for KAO, MK and GEO.7 respectively and then it becomes nearly constant. The 15 min corresponds to both equilibrium time of MO uptake by KAO and GEO.7 which was similar to the result obtained by Karimi *et al.* (2012) during the removal of MO using the activated charcoal.

Fig. 4. Effect of agitation time on the adsorption of MO on KAO, MK and GEO.7.

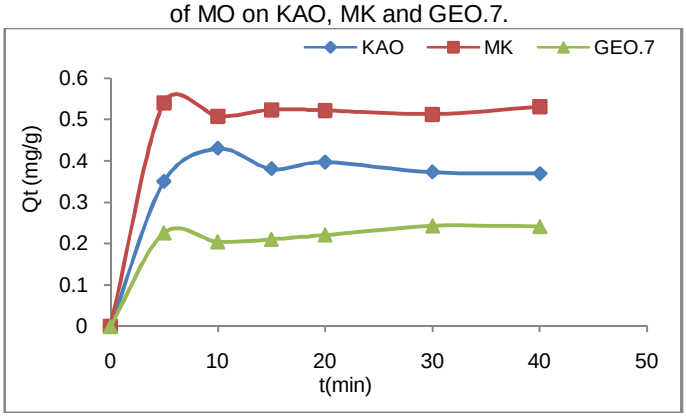

Effect of adsorbents dosage: The typical results in Fig. 5 show that for an increase in each adsorbent dosage, the adsorbent sites available upon the dye molecules also increase and consequently poor adsorption. This is due to electrostatic attraction forces between particles that constitute the surface of adsorbents, the decrease of molecular diffusion of the MO. Another consequence is the reduction of activated sites at the surface of the adsorbents and also the matter rate transfer of MO at the surface of the adsorbents, this means that the quantity of MO adsorbed per unit mass of adsorbent has it limit with the adsorbent dosage. Similar result has been obtained by Rajesh *et al.* (2010) during the removal of malachite green using *Hydrilla Verticillate* biomass.

Fig. 5. Effect of adsorbent dosage on MO adsorption; C_o= 20 mg/L; pH = 2.5.

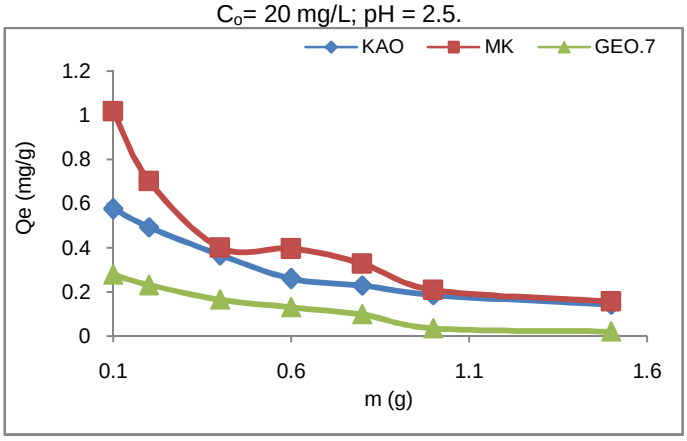

Effect of pH: The pH of solution is an important factor in the adsorption process, which may alter the surface properties of the adsorbents as well as the degree of ionization and the speciation of the dye (Yavuz and Aydin, 2006). The influence of pH on the MO adsorption onto KAO, MK and GEO.7 was studied for the dye concentration (20 mg/L) and amount of adsorbents (100 mg/20 mL) in the pH range of 2.5-9 with the results shown in Fig. 6. The lower pH of solution has more influence on adsorption. MO is an anionic acid dye as denoted by the presence of the negative sulfonate ion (SO_3^-) in its structure.

In present study, with the pH 2.5 the quantity of the adsorbed MO was high, this might be due to the influence of the H^+ cation on micelle of the clays, which causes attraction of the negatively charge dye. The sorption capacity at equilibrium then decreased as pH increased from 3.5 to 9 due to the increase of the negative charges on the surface of adsorbents. The consequence is the decrease of diffusion and uptake of MO due to high electrostatic forces repulsion. GEO.7 adsorption capacity of MO was very weak due to its basic nature. This included the great competition between MO and hydroxyl ion (OH^-) on the sorption sites. Similar result was obtained by Ozcan and Ozcan (2004) and Lim *et al*. (2010) during the removal of acid dyes onto acid activated bentonite. The value 2.5 was chosen to perform the equilibrium and kinetic studies.

Fig. 6. Effect of pH solution on MO adsorption on KAO, MK and GEO.7.

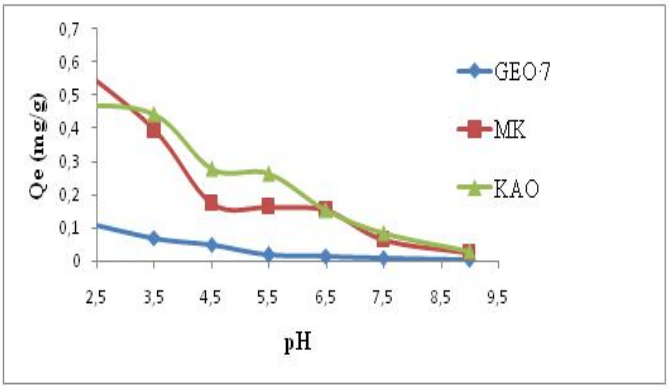

Adsorption isotherms: Table 2 gives different values of the constants obtained from the three isotherm models which were used to describe our experimental data. It also shows that the experimental data fitted Langmuir better than Freundlich and D-K-R isotherm equation by comparing their R^2 values. Figure 7 shows the adsorption isotherms of MO. In this case, on both KAO and GEO.7, they are of type II type I on MO adsorption. It characterizes non-porous solids. The linear plots of Langmuir, Freundlich and D-K-R are shown in Figs. 8, 9 and 10.

Table 2. Results of various isotherm plots for the adsorption of MO onto KAO, MK and GEO.7.

Isotherm models	Parameters	Adsorbents		
		KAO	MK	GEO.7
Langmuir	R^2	0.984	0.995	0.972
	Q_{max}(mg/g)	1.247	3.076	3.076
	K_L (L/g)	0.012	0.032	0.026
Freundlich	R^2	0.970	0.984	0.984
	1/n	0.908	1.432	1.890
	K_f (L/g)	0.04	0.023	0.002
D-K-R	R^2	0.797	0.920	0.785
	Q_{max}(mg/g)	0.805	1.498	0.720
	E_a (KJ/mol)	0.006	0.009	0.005

Fig. 7. Adsorption isotherms of MO on KAO, MK and GEO.7; C_o = 20 mg/L.

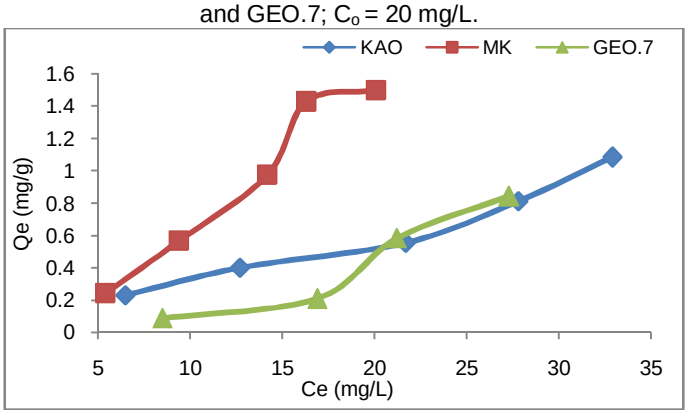

Fig. 8. Linear plots of Langmuir model C_o= 20 mg/L; m=0.1 g; pH=2.5.

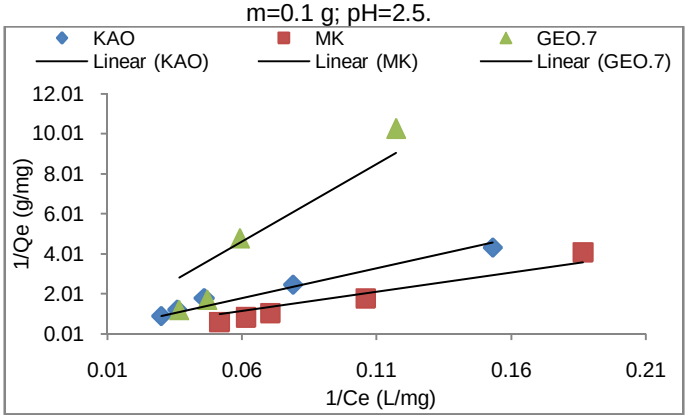

Fig. 9. Linear plots of Freundlich model C_o = 20 mg/L; m=0.1 g; pH = 2.5.

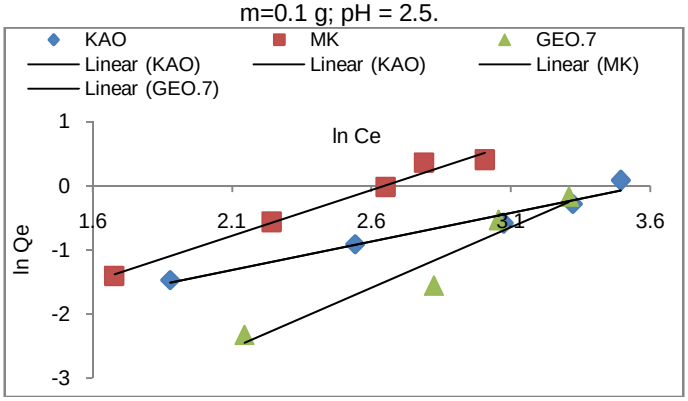

Fig. 10. Linear plots of D-K-R model C_o = 20 mg/L; m = 0.1 g; pH = 2.5.

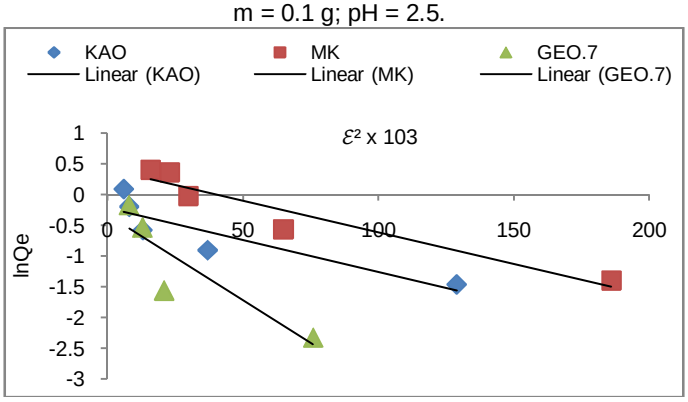

Fig. 11. Pseudo first order plots for MO adsorption on KAO, MK and GEO.7; C_o = 20 mg/L; pH = 2.5.

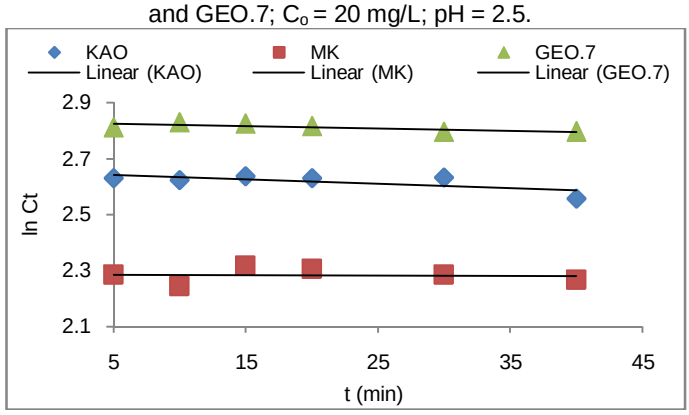

Fig. 12. Pseudo second order plots for MO adsorption on KAO, MK and GEO.7; C_o = 20 mg/L; pH = 2.5.

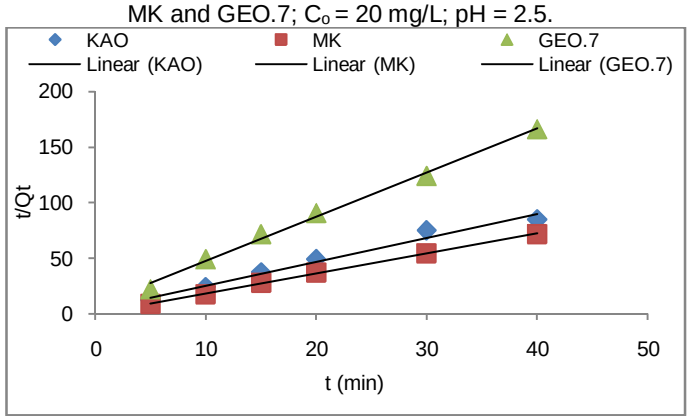

Fig. 13. Mass transfer plots for MO adsorption on KAO, MK and GEO.7; C_o= 20 mg/L; pH = 2.5.

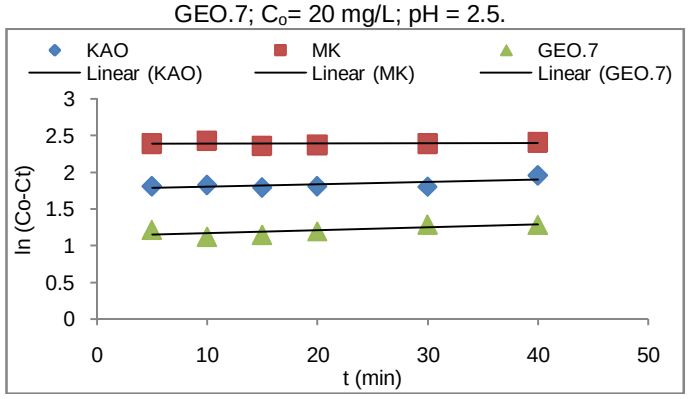

Fig. 14. Elovich plots for MO adsorption onto KAO, MK and GEO.7; C_o= 20 mg/L; pH = 2.5.

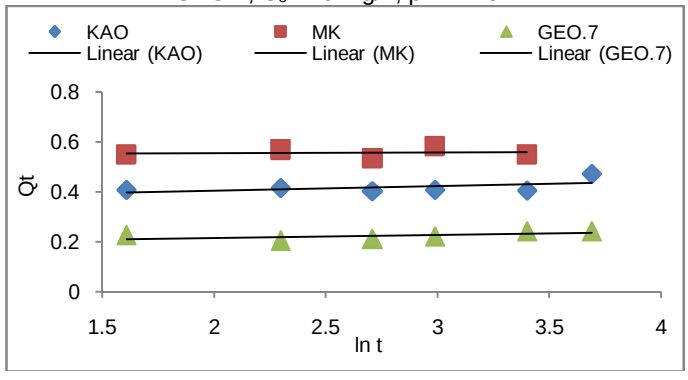

Fig. 15. Intraparticle diffusion plots for MO on KAO, MK and GEO.7; C_o= 20 mg/L; pH = 2.5.

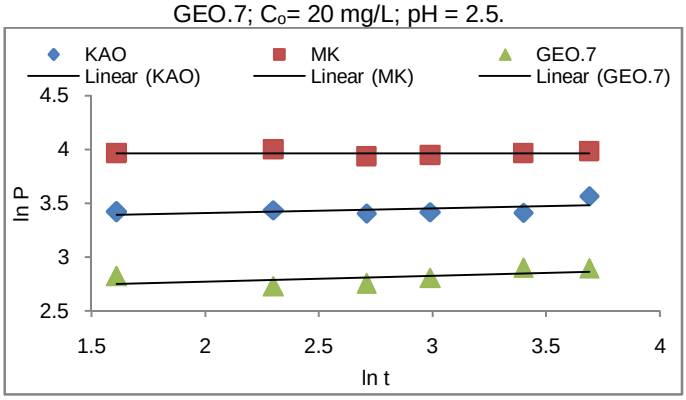

Table 3. Calculated kinetic parameters for the adsorption of MO onto KAO, MK and GEO.7.

Kinetic models	Parameters	Adsorbents		
		KAO	MK	GEO.7
Pseudo first order	R^2	0.494	0.004	0.571
	ln C_o	2.650	2.285	2.828
	$K_1.10^{-3}(min^{-1})$	1.000	0.000	0.001
Pseudo second order	R^2	0.982	0.999	0.996
	h(mg/g.min)	0.249	1.439	0.774
	K_2(g/mg.min)	1.142	0.921	7.340
	$Q_e$exp(mg/g)	0.402	0.568	0.209
	$Q_e$cal(mg/g)	0.467	0.556	0.225
Elovich	R^2	0.281	0.001	0.346
	β(g/mg)	$1.2.10^{7}$	250	83.33
	α(mg/g.min	55.56	7.10^{-5}	8.10^{3}
Intraparticle diffusion	R^2	0.262	0.001	0.339
	$K_{id}(min^{-1})$	27.88	29.05	14.39
	a (mg/g)	0.041	- 0.001	0.053
Mass transfer	R^2	0.483	0.004	0.555
	$K_o(min^{-1})$	3.050	0.000	0.004
	ln D	1.770	2.935	1.128

Kinetics of adsorption: The kinetic studies describe the rate of adsorption and this rate controls the equilibrium time. These kinetic models are useful for the design and optimization of effluent models. Pseudo first order, pseudo second order, Elovich, intraparticle diffusion and mass transfer kinetic models were analyzed for the mechanism of MO adsorption by KAO, MK and GEO.7. The straight-line plots are presented in Figs.11 to 15 and the results are presented in (Table 3). The pseudo second order rate constant decreases with increase in initial concentration. The determining values of Q_e calculated from the equation differ from the experimental values, which show the adsorption of MO onto KAO, MK and GEO.7 fitted better to the pseudo second order kinetic model according to correlation coefficient value, R^2>0.98, this implies that MO removal on the three adsorbents may occur through a chemical process involving the valence forces (Essomba *et al.,* 2014). This also means that chemisorption is the limiting step.

Conclusion

The present study revealed that kaolinite, metakaolinite and activated geopolymer derived from kaolin can be used as low-cost adsorbents for the removal of MO from aqueous solution. Adsorption was high in acidic conditions at pH 2.5. As the adsorbents dosage increased, a decrease in MO removal was observed, and the adsorption capacity increased with increasing initial MO concentration. The experimental data fitted well Langmuir isotherm and pseudo second order kinetic model. Dye uptake efficiency Q_e was found to increase in the following order MK>KAO>GEO.7.

Acknowledgements

Authors thank all the members of the research group “Adsorption and Surface”, of Physical and Theoretical Chemistry Laboratory and Pr. Antoine Elimbi of the Material Science Laboratory of the University of Yaoundé I for their remarks and suggestions.

References

1. Abdullah, A.G., Mohd Sallah, M.A., SitiMazlina, M.K., Megat Mohd Noor, M.J., Osman, M.R., Wagiran, R. and Sobri, S. 2005. Azodye removal by adsorption using waste biomass: Sugarcane bagasse. *Int. J. Engg. Technol*. 2(1): 8-13.
2. Albanis, T.A., Hela, D.G., Sakellarides, T.M. and Danis, T.G. 2000. Removal of dyes from aqueous solutions by adsorption on mixtures of fly ash and soil in batch and column techniques. *Global Nest Int. J.* 2(3): 237-244.
3. Ali, I. and Jain, C.K. 2005. In water Encyclopedia: Domestic, Municipal, and Industrial water supply and waste disposal (Ed. Lehr, J.) John wiley & Sons, New York.
4. Almutairi, F.M., Williams, P.M. and Lovitt, R.W. 2012. Effect of membrane surface change on filtration of heavy metal ions in the presence and absence of polyethylenimine. *Desalinat. Water Treat.* 42: 131-137.
5. Anagho, G.S., Mbadcam, J., Tchuifon, D.R. and Ndi, N.J. 2013. Kinetic and equilibrium studies of the adsorption of the mercury (II) ions from aqueous solution using kaolinite and metakaolinite clays from Southern Cameroon. *Int. J. Res. Chem. Environ.* 3(2): 1-11.
6. Augustine, A.A., Orike, B.D. and Edidiong, A.D. 2007. Adsorption kinetics and modeling of Cu(II) ion sorption from aqueous solutions by mercaptoacetic acid modified cassava (*manihotsculentacranz*) wastes. *Electron. J. Environ. Agric. Food. Chem.* 6(4): 2221-2234.
7. Crini, G. 2006. Non-conventional low-cost adsorbents for dye removal: A review. *Bioresour. Technol.* 97(9): 1061-1085.
8. Elimbi, A., Tchakouté Kouamo, H. and Njopwouo, D. 2011. Effects of calcination of kaolinite clays on the properties of geopolymer cements. *Constr. Build. Mater.* 25: 2805-2812.
9. Essomba, J.S., Ndi Nsami, J., Bélibi Bélibi, P.D., Tagne, G.M. and Ketcha Mbadcam, J. 2014. Adsorption of cadmium(II) ions from aqueous solution onto kaolinite and metakaolinite. *Pure. Appl. Chem. Sci.* 2(1): 11-30.

10. Gong, R., Jin, Y., Chen, F., Chen, J. and Lui, Z. 2006. Enhanced malachite green removal from aqueous solution by citric acid modified rice straw. *J. Hazard. Mater.* 137: 865-870.
11. Hameed, B.H. 2007. Equilibrium and kinetic studies of methyl violet sorption by agricultural waste. *J. Hazad. Mater.* 154(1-3): 204-212.
12. Imran, A. and Gupta, V.K. 2006. Advances in water treatment by adsorption technology. *Nat. Prot*. 1(6): 2661-2667.
13. Karimi, H., Moussovi, S. and Sedeghian, B. 2012. Silver nanoparticle loaded on activated carbon as efficient adsorbent of removal of methyl orange. *Ind. J. Sci. Technol*. 5(3): 2346-2353.
14. Lim, H.Y., Vinoth, M., Xavier, R., Marimuth, K., Screeraman, S., Wes Rasemal, H. M.H. and Ketchiresen, S. 2010. Removal of methyl orange from aqueous solution using yam leaf fibers. *Int. J. Chem. Technol. Res*. 2(4): 1892-1900.
15. Mbadcam, J.K., Dogmo, S. and Dinka'a Ndaghu, D. 2012. Kinetic and thermodynamic studies of the adsorption of nickel (II) ions from aqueous solution by smectite clay from Sabga-Cameroon. *Int. J. Curr. Res.* 4(5): 162-167.
16. Mohammed, S., Alireza, M., Amir, H., Mahvi, S., Simin, N. and Ramin, N. 2012. Kinetics and equilibrium studies on adsorption of acid red 18 (azo-dye) using multiwall carbon nanotubes from aqueous solution. *Euro. J. Chem*. 9(4): 2371-2383.
17. Nacera,Y. and Bensmaili. 2005. Kinetic models for the sorption of dye from aqueous solution by clay-wood sawdust mixture. *Desalinat*. 185: 499-508.
18. Nsami, J.N. and Mbadcam, J.K. 2013. The adsorption efficiency of chemically prepared activated carbon from cola nut shells by $ZnCl_2$ on methylene blue.*Hind. Publish. Corporat. J. Chem.* 2013: 1-7.
19. Ozcan, A.S. and Ozcan, A. 2004. Adsorption of acid dyes from aqueous solution onto acid activated bentonite. *J. Colloid. Interface. Sci.* 276: 39-46.
20. Pierce, J. 1994. Colour in textile effluent-the origin of the problems. *J. Soc. Dyers. Colour*. 110: 131-134.
21. Raffeia, B.J., Polanisamy, P.N. and Siva Kumar, P. 2012. Adsorption of basic dyes from synthetic textile effluent by activated carbon prepared from *Thevetiaperuviana. Ind. J. Chem. Technol*. 19: 311-321.
22. Rajesh, K.R., Rajasimman, M., Rajamohan, N. and Sivaprokash, B. 2010. Equilibrium and kinetics studies on sorption of malachite green using *Hydrilla verticillate* biomass. *Int. J. Environ. Res*. 4(4): 817-828.
23. Ramaraju, B., Kumar, P.M. and Subrahmanyan, C. 2013. Low cost adsorbents from agricultural waste removal of dyes. *Environ. Prog. Sustain. Energ*. 33(1): 38-46.
24. Saikia, J.B. and Parasarathy, G. 2010. Fourier transform infrared spectroscopic characterization of kaolinite from Assam and Meghalaya, North Eastern India. *J. Modern. Phys*. 1: 2006-2010.
25. Samarghandi, M.R., Hadi, M., Moayedi, S. and Barjesteh, A.F. 2009. Two parameter isotherms of methyl orange by pinecone derived activated carbon. *Iran. J. Environ. Health. Sci. Engg.* 6(4): 285-294.
26. Smaranda, C., Gravilescu, M. and Bulgrin, D. 2011. Studies on sorption of congo red from aqueous solution onto soil. *Int. J. Environ. Res.* 5(1): 177-188.
27. Supdita, C. 2010. Adsorption of congo red by chitosan hydrogel beads impregnated with carbon nanotube. *Bioresour. Technol*. 101: 1800-1806.
28. Theivarasu, C., Mylsamy, S. and Sivakumar, N. 2011. Removal of Malachite Green from Aqueous Solution by Activated Carbon Developed from Cocoa (*Theobroma cacao*) Shell: Kinetic and Equilibrium Studies. *Orient. J. Chem*. 27(3): 1083-1091.
29. Voudrias, E., Fytianos, K. and Bozani, E. 2002. Sorption-desorption isotherms of dyes from aqueous solutions and wastewaters with different sorbent materials. *Global Rest Int. J*. 4(1):72-82.
30. Yavuz, O. and Aydin, A.H. 2006. Removal of direct dyes from aqueous solutions using various dyes. *Pol. J. Environ. Studies*. 15(1): 155-161.
31. Zhang, T., Wang, Y., Ng, J. and Sun, D.D. 2012. A free-standing, hybrid TiO_2, K-OMS-2 hierarchical nanofibers membrane with high photocatalytic activity for concurrent membrane filtration applications. *RSC. Adv*. 2: 3636-3641.
32. Zora, M. and Snezena, B. 2006. Kinetic studies and spectrophometric determination of Co(II) ions by the oxidation of poncean by hydrogen peroxide. *J. Serb. Chem. Soc.* 71(2): 181-196.